Ultrabroadband detection of a mid-IR continuum by chirped-pulse upconversion

Carlos R. Baiz and Kevin J. Kubarych*

Department of Chemistry, University of Michigan, Ann Arbor, Michigan 48109, USA
**Corresponding author: kubarych@umich.edu*

Received November 19, 2010; accepted December 2, 2010;
posted December 8, 2010 (Doc. ID 138513); published January 11, 2011

Ultrabroadband mid-IR continuum pulses can be detected on a single-shot basis using chirped-pulse upconversion. Converting the mid-IR pulse to the visible reduces the fractional bandwidth and enables use of a silicon CCD camera. Removing the cross-phase modulation of the chirped pulse results in 1 cm^{-1} resolution over a 600 cm^{-1} detected bandwidth. © 2011 Optical Society of America

OCIS codes: 190.7220, 190.4380, 190.2620, 320.6629.

Over the past decade, IR spectroscopy on the subpicosecond timescale has provided remarkable insights into fundamental processes in chemistry and biology, from bond formation [1], dissociation [2], and isomerization [3], to protein folding [4] and aggregation.[5] Unlike conventional Fourier-transform spectroscopy, ultrafast mid-IR spectroscopy has been limited to small spectral windows of widths typically <500 cm^{-1}, where only a small set of nearby vibrations can be measured simultaneously.[6] Ideally, ultrafast spectroscopy with IR pulses should be able to access the entire 500–4000 cm^{-1} spectral region, providing maximum structural and dynamical information. Two constraints limit the spectral bandwidth of IR generation and detection. Firstly, conventional implementations rely on optical parametric amplification (OPA) followed by difference frequency generation (DFG) to produce mid-IR pulses and are limited in bandwidth by phase matching [7]. Secondly, direct multichannel IR detection is carried out using mercury–cadmium–telluride (MCT) detector arrays that suffer from low pixel count, reduced sensitivity, and high cost compared to their silicon-based counterparts for visible detection. A state-of-the-art MCT detector features only 128 pixels.

Broadband sources of terhertz and mid-IR radiation through plasma generation in air have been recently demonstrated [8–12]. In particular, Petersen and Tokmakoff implemented a new IR continuum source for sub-100 fs pulses spanning <400 cm^{-1} to >3000 cm^{-1} by simultaneously focusing three high-intensity pulses centered at 800, 400, and 267 nm in air [13]. Though the complete mechanism of the IR continuum generation is not yet well understood, the process has been described in terms of optical rectification [8,9] in collisional plasma [14]. Until now, the efficient detection of such a continuum source has remained a challenge. In this Letter, we describe a straightforward apparatus for ultrabroadband mid-IR generation and detection based on chirped-pulse upconversion [15,16] (CPU), whereby starting with 100 fs 800 nm pulses, we can achieve a nearly 1000 cm^{-1} detected bandwidth with 1 cm^{-1} spectral resolution over most of the mid-IR (1600 to 4100 cm^{-1}).

The optical setup is illustrated in Fig. 1. Pulses derived from a 100 fs 2 mJ Ti:sapphire amplifier (Spectra-Physics Spitfire Pro) are split in a 50:50 ratio. One half is used for IR generation, while the other half is used for upconversion. Since the bandwidth of the IR continuum is dictated by the bandwidth of the source, we spectrally broaden the 800 nm pulse via self-phase modulation in argon [17]. The 1 mJ 800 nm pulses are focused using a $f =$ 50 cm lens into a 125 μm hollow-core fused silica fiber (Femtolasers OA219) placed inside a pressurized chamber. The 400 μJ fiber output is collimated to a diameter of 5 mm and recompressed using a pair of 1.5 in. fused silica Brewster prisms. Typically, 40 fs FWHM compressed pulses are obtained with 0.75 atm of Ar and a 234 cm tip-to-tip prism-pair distance. The compressed pulses are sent through an in-line second and third-harmonic-generation setup [18]. Second harmonic pulses are generated by type I phase matching in a 0.4 mm beta-barium borate (BBO) crystal, followed by a calcite plate (Eksma 225-2112) to compensate the group delay of the entire setup (83 fs BBO +451 fs waveplate +220 fs BBO). Next, a dual-band $\lambda/2$ waveplate (Eksma 466–4211) rotates the 800 nm polarization to coincide with the 400 nm polarization. Finally, type I sum-frequency generation in a 0.4 mm BBO generates the 267 nm third harmonic. The three pulses are focused into air using a spherical dielectric mirror with a 10 cm radius (Layertec 100600). A bright ~0.5 mm filament is observed at the focus, and the IR continuum intensity correlates well with the brightness of the filament. A 12 cm radius aluminum-coated spherical mirror collimates the light, and a 1 mm Ge window filters out the UV and visible light. The IR is then refocused to a ~1 mm spot using a 12 cm spherical gold-coated mirror. The total IR output is measured and optimized by placing a single-channel MCT detector (IR Associates MCT-20-1.0) at the focus; after attenuation by an OD = 0.3 neutral density filter, the IR power is still sufficient to saturate the detector. A sample of $Mn_2(CO)_{10}$ in cyclohexane provides narrow absorption bands in the carbonyl stretching region (~2000 cm^{-1}) to calibrate the detection axis, test the phase-correction procedure, and evaluate the effective spectral resolution of the upconversion. The remaining 1 mJ of 800 nm laser output is sent through a grating stretcher constructed from a 1200 grooves/mm grating (Spectrogon 9800–2840). Finally, the ~15 ps chirped pulses (350 μJ) are mixed with the IR continuum in a type I SFG arrangement using a wedged 0.3-to-0.8 mm MgO(5%):LiNbO3 (LNB) crystal. The leftover 800 nm is filtered out by a 750 nm

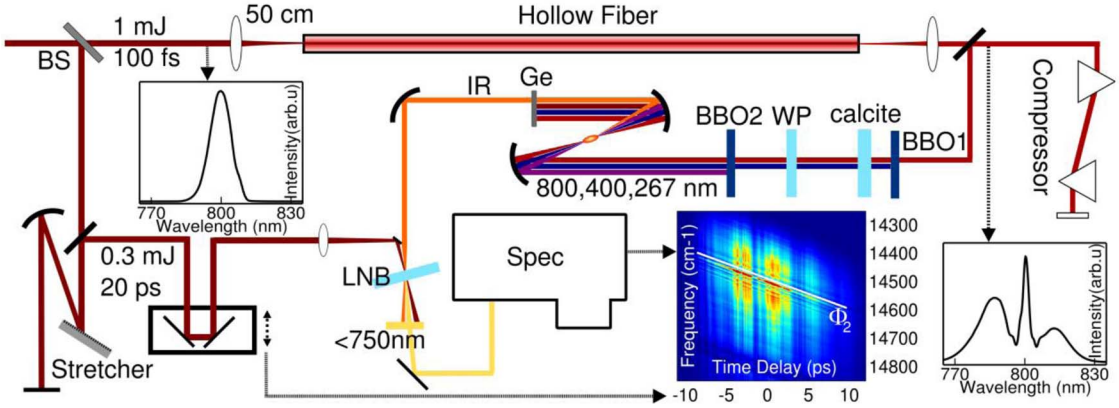

Fig. 1. (Color online) IR continuum generation and upconversion setup. Spectra corresponding to the 800 nm pulses before and after the hollow fiber are shown for comparison. A spectrogram of the upconverted IR as a function of the IR-800 delay shows the second-order spectral phase of the 800 nm chirped pulse.

shortpass filter and sent to a conventional visible spectrometer equipped with a 1340 × 100 pixel CCD detector (Pixis, Princeton Instruments) that can be operated in a mode that can record 1340 pixel spectra at 1 kHz. Unless focused, the upconverted visible light (~650 nm) cannot be seen by the naked eye; thus a small 4° angle between the IR and 800 nm beams ensures that the upconverted light will be practically collinear with the 800 nm beam, which facilitates its initial alignment into the spectrometer.

The IR source is particularly stable; the measured shot-to-shot noise percentage (standard deviation/mean) of the IR continuum is 2.0% (upconverted) or 3.1% (MCT), which compares well with a 0.7% shot-to-shot noise in our OPA-DFG narrowband IR generation setup pumped by the same laser. In terms of the total IR bandwidth, we were able to upconvert frequencies between 1600 and 4100 cm^{-1}, indicating that the continuum spans the entire mid-IR region. The low-frequency limit is due to IR absorption in LNB and can be circumvented using other nonlinear media. To measure the continuum generation efficiency in different gases, N_2, CO_2, and Ar were flowed from a nozzle placed 2 mm below the plasma filament. The IR intensity increase relative to that in air measured using the MCT is as follows: 7% (N_2), 17% (CO_2), and 24% (Ar). We measured the bandwidth changes by simultaneously upconverting two IR regions centered at 1646 (type I) and 3114 (type II) cm^{-1} in a single LNB crystal. The high- to low-frequency intensity ratios are 1.1 (N_2), 2.0 (CO_2), 2.2 (Ar), normalized to a 1.0 ratio in air, suggesting that increasingly polarizable gases can enhance the generated IR intensity at the high-frequency region, consistent with recent THz generation studies [19].

A frequency-resolved cross-correlation between the IR and upconverting pulses measures the instantaneous frequency and amplitude of the chirped pulse (CP). Since no optical realignment is required, the chirp characterization can be performed *in situ* by scanning the time delay between the two pulses. When no attempt is made to remove the cross-phase modulation imparted by the chirped pulse, the resulting spectrum is convolved with the bandwidth present during overlap with the mid-IR pulse. Here, the continuum pulse is measured to have a temporal width of 58 fs FWHM by cross-correlation (SFG) with a transform-limited 100 fs 800 nm pulse. Thus, the uncorrected CPU spectral convolution is 0.5 cm^{-1}, given that the CP has an FWHM bandwidth and a duration of 130 cm^{-1} and 15 ps, respectively. By comparison, upconversion with a transform-limited 15 ps Gaussian pulse would be convolved with 1.1 cm^{-1}. In addition to the spectral convolution, the second-order phase of the CP modulates the phase of the upconverted IR pulse and causes severe distortions when narrow absorption lines are present. Correcting for these distortions and recovering the original lineshapes is straightforward.[20,21] In brief, a power spectrum is Fourier-transformed into the time domain where the antisymmetrized second-order phase is divided out and the spectrum is inverse Fourier-transformed back into the frequency domain. The phase can be recovered from the cross-correlation by extracting the value of the upconverted frequencies as a function the CP-IR delay (see spectrogram in Fig. 1). The first-order phase, or absolute IR-CP delay, is not precisely known, and thus there is an ambiguity in the absolute frequency. This can be

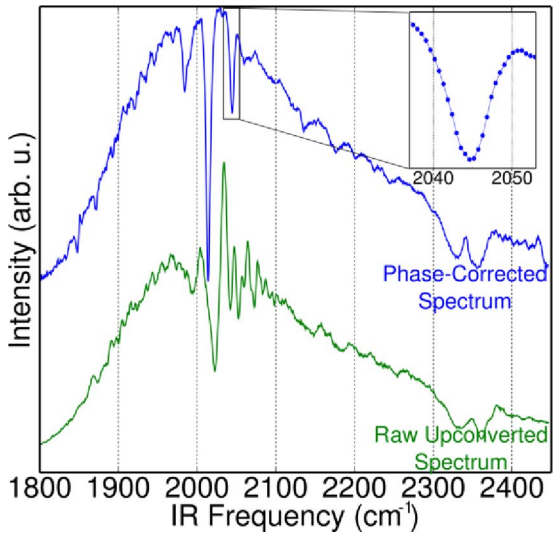

Fig. 2. (Color online) Upconverted IR continuum. The absorption lines at 1983, 2013, and 2045 cm^{-1} correspond to carbonyl stretches in $Mn_2(CO)_{10}$; the remaining absorption lines are from atmospheric water and carbon dioxide. The inset shows the large number of points measured by upconversion. The spectra are collected with an integration time of 100 ms.

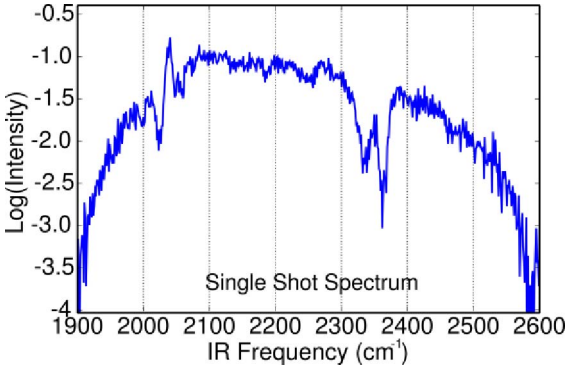

Fig. 3. (Color online) Single-shot upconverted IR spectrum (not phase corrected). The peaks near 2350 cm^{-1} correspond to absorption by atmospheric carbon dioxide.

corrected by shifting the frequency axis to reproduce the known transition frequencies of a reference sample. Raw upconverted and corresponding phase-corrected spectra are shown in Fig. 2. The narrow peaks of $Mn_2(CO)_{10}$ (6.5 cm^{-1} FWHM) are recovered by the phase correction procedure with no loss of spectral resolution. Given a chirped pulse long enough to match the longest free-induction decays (narrowest transitions), the spectral resolution is only determined by how accurately the second-order phase can be measured. Although upconversion can also be implemented using a narrowband pulse, from a practical perspective, the chirped-pulse upconversion method efficiently uses all the light available, whereas to attain a 1 cm^{-1} narrowband pulse starting from a 100 fs pulse, >99% of the light must be discarded through spectral filtering. This is an important advantage of the CPU method. Finally, another advantage of upconversion over direct IR detection lies in its ability to simultaneously detect a full octave of IR bandwidth, whereas overlapping diffraction orders from the grating would prevent direct detection in the IR unless additional filters are placed after the grating.

Signal intensity versus bandwidth is the central trade-off within CPU: a thin upconversion crystal will support a broader bandwidth, but with less conversion efficiency, and thus a low-noise detector is essential to achieving ultrabroadband upconversion. To measure the signal-to-noise ratio and detection limit of the setup, we collected single-shot spectra (Fig. 3). Near the most intense region (~2200 cm^{-1}), the detector noise to signal intensity ratio is 1.3% (~10^{-2} OD), a value comparable to the shot-to-shot fluctuations. A high pixel density (~2 pixels/cm^{-1}), means that a low-pass filter can be applied to further reduce the noise without significant loss of spectral resolution.

In conclusion, we have demonstrated an ultrabroadband generation and detection method based on chirped-pulse upconversion that spans the complete mid-IR region. The detection bandwidth is limited only by the thickness of the nonlinear crystal and the spectrometer noise. We believe that the developments presented here will find immediate applications in transient absorption and multidimensional IR spectroscopy.

This project was supported by the National Science Foundation (NSF) (CHE-0748501; K. J. Kubarych), as well as a graduate student research grant and predoctoral fellowship from the Rackham Graduate School at the University of Michigan (C. R. Baiz). We thank Steve Donajkowski for building the pressurized fiber chamber.

References

1. C. R. Baiz, R. McCanne, and K. J. Kubarych, J. Am. Chem. Soc. **131**, 13590 (2009).
2. P. A. Anfinrud, C. Han, and R. M. Hochstrasser, Proc. Natl. Acad. Sci. USA **86**, 8387 (1989).
3. J. R. Zheng, K. W. Kwak, J. Xie, and M. D. Fayer, Science **313**, 1951 (2006).
4. Z. Ganim, K. C. Jones, and A. Tokmakoff, Phys. Chem. Chem. Phys. **12**, 3579 (2010).
5. S. H. Shim, R. Gupta, Y. L. Ling, D. B. Strasfeld, D. P. Raleigh, and M. T. Zanni, Proc. Natl. Acad. Sci. USA **106**, 6614 (2009).
6. M. Cho, *Two-Dimensional Optical Spectroscopy* (CRC Press, 2009)
7. R. A. Kaindl, M. Wurm, K. Reimann, P. Hamm, A. M. Weiner, and M. Woerner, J. Opt. Soc. Am. B **17**, 2086 (2000).
8. D. J. Cook and R. M. Hochstrasser, Opt. Lett. **25**, 1210 (2000).
9. T. Fuji and T. Suzuki, Opt. Lett. **32**, 3330 (2007).
10. M. D. Thomson, V. Blank, and H. G. Roskos, Opt. Express **18**, 23173 (2010).
11. J. L. Liu, J. M. Dai, S. L. Chin, and X. C. Zhang, Nat. Photon. **4**, 627 (2010).
12. A. A. Silaev, M. Yu. Ryabikin, and N. V. Vvedenskii, Phys. Rev. A **82**, 033416 (2010).
13. P. B. Petersen and A. Tokmakoff, Opt. Lett. **35**, 1962 (2010).
14. J. Penano, P. Sprangle, B. Hafizi, D. Gordon, and P. Serafim, Phys. Rev. E **81**, 026407 (2010).
15. K. J. Kubarych, M. Joffre, A. Moore, N. Belabas, and D. M. Jonas, Opt. Lett. **30**, 1228 (2005).
16. M. J. Nee, R. McCanne, K. J. Kubarych, and M. Joffre, Opt. Lett. **32**, 713 (2007).
17. M. Nisoli, S. DeSilvestri, and O. Svelto, Appl. Phys. Lett. **68**, 2793 (1996).
18. H. Enqvist, *Lund Reports on Atomic Physics*, Vol. 330 (Lund University, 2004).
19. G. Rodriguez and G. L. Dakovski, Opt. Express **18**, 15130 (2010).
20. K. F. Lee, P. Nuernberger, A. Bonvalet, and M. Joffre, Opt. Express **17**, 18738 (2009).
21. J. M. Anna, M. J. Nee, C. R. Baiz, R. McCanne, and K. J. Kubarych, J. Opt. Soc. Am. B **27**, 382 (2010).